

Rotational effect in two-dimensional cooperative directed transport

Li-Yan Qiao¹, Yun-yun Li², Zhi-Gang Zheng^{1,†}

¹*Department of Physics and the Beijing-Hong Kong-Singapore Joint Center for Nonlinear and Complex Studies, Beijing Normal University, Beijing 100876, China*

²*Center for Phononics and Thermal Energy Science, School of Physics Science and Engineering, Tongji University, Shanghai 200092, China*

Corresponding author. E-mail: †zgzheng@bnu.edu.cn

Received March 7, 2014; accepted April 10, 2014

In this review we investigate the rotation effect in the motion of coupled dimer in a two-dimensional asymmetric periodic potential. Free rotation does not generate directed transport in translational direction, while we find it plays an critical role in the motors motility when the dimer moves under the effect of asymmetry ratchet potential. In the presence of external force, we study the relation between the average current and the force numerically and theoretically. The numerical results show that only appropriate driving force could produce nonzero current and there are current transitions when the force is large enough. An analysis of stability analysis of limit cycles is applied to explain the occurrence of these transitions. Moreover, we numerically simulate the transport of this coupled dimer driven by the random fluctuations in the rotational direction. The existence of noise smooths the current transitions induced by the driving force and the resonance-like peaks which depend on the rod length emerge in small noise strength. Thanks to the noise in the rotational direction, autonomous motion emerges without the external force and large noise could make the current reversal happen. Eventually, the new mechanism to generate directed transport by the rotation is studied.

Keywords molecular motor, rotational effect, noise, rotation-translation coupling, directed translational motion

PACS numbers 87.16.Nn, 87.17.Aa, 05.40.-a

Contents

| | |
|---|--------------------------------|
| 1 | Introduction |
| 2 | Rotation-translation coupling |
| 3 | Deterministic current behavior |
| 4 | Stochastic dynamic behavior |
| 5 | Conclusions |
| | Acknowledgements |
| | References |

filaments, carrying out essential tasks such as organelle transport [1–5].

1 Katsuyuki Shiroguchi and his co-workers proved that
2 there is rotational motion when myosin V walks along
3 the actin filament by experiment [6]. Also the leading
4 neck swings unidirectionally forward, whereas the trail-
5 ing neck, once lifted, undergoes extensive Brownian ro-
6 tation in all directions before landing on a site ahead of
7 the leading head. Dunn found that the unbound head
8 rotate freely about the lever-arm junction as it releases
9 from the actin filament. Also translational motion of a
10 neck during the transients was reported in his work [7].
11 Extensive single molecule experiments have emphasized
12 the importance of the translational movement of the neck
13 and the rotational motion of the arm during the “hand-
14 over-hand” mechanism.

Molecular motors convert chemical energy from ATP hydrolysis into mechanical and/or chemical work during

1 Introduction

The mechanisms of molecular motor in cooperative directed transport have been the subject of much attention, ranging from biophysics, chemistry and biomedical research for several decades. In the last few years biologists have found that most of the motor proteins literally walk, in a “hand-over-hand” fashion, along polymeric

this process in a very efficient way [8]. The correspondence between the conformational change in the neck of ATP hydrolysis consumption and their contribution to the motor protein motility has been a major research topic. From a theoretical point of view, molecular motors are microscopic objects that unidirectionally move along one-dimensional periodic structures. Understanding this active system, which is constantly driven away from the thermodynamics equilibrium, has been a challenge for physicists, biologists, and chemists. Therefore, the study of stochastic dynamics of molecular machines is often based on simple models that describe these complex biomolecules as single-coordinate ratchets or oscillators [9, 10]. A number of investigations have been made in the past few years on theoretical models based on those most basic motility mechanism [11–15].

Recently researchers try to pay more attention on the effect of the directed transport due to the structural dynamics of motor molecules which are typically dimeric [16]. Some researchers suppose the dimer consists of two harmonically coupled components and theatchet effect is caused by the internal degree of freedom, an interaction between the components of the dimer, such as the work from Gehlen *et al.* [17] or the current may be obtained via a pulling effect in a flashing ratchet potential [18]. While some physical scientists prefer to consider a motor particle as a simple rod which converts rotational diffusion into directed translational motion by switching on and off a potential [19]. However, little work has attempted to simulate the effect of periodic rotation and neither of them have consider the translational motion due to the fluctuation in the rotational direction.

In the present paper, we go further the latter model in exploring and understanding the essential features of the motor system. We also consider that the rod is connected with two identical heads and could rotate around the mass of center. Free rotation does not generate translational motion, while we find it plays an critical role in the motors motility when the dimer moves in the plane under the effect of asymmetry ratchet potentials. The main motivation behind this work is to study in detail the directed transport in the x direction induced by the rotation effect of the model. A point worth emphasizing is that there is no external force (even noise) drive the system in translational dimension. The rotational effect mechanism could transfer the energy from one dimension to another and realize the directed motion in asymmetric periodic potential. The instability induced by the rotation makes the system need longer time to get directed current. Moreover, we do not consider the behavior of any single head and focus on the kinematics of the mass of center and the rotational motion of the dimer.

The paper is arranged as follows. In Section 2, we propose the system with translational and rotational degrees of freedom to describe the model. We present results for our model in the deterministic regime, varying the external force in the rotational direction in Section 3 and the behaviour of the current in the presence of thermal noise in Section 4. Our conclusions are contained in Section 5.

2 Rotation-translation coupling

In the present work, we consider a dimer which consists of two identical globular motors connected with a simple rod of length l whose degrees of freedom are defined as the position of the center of mass x and a rotational angle θ around the center [19]. The motor is free to thermally diffusion in both x and θ .

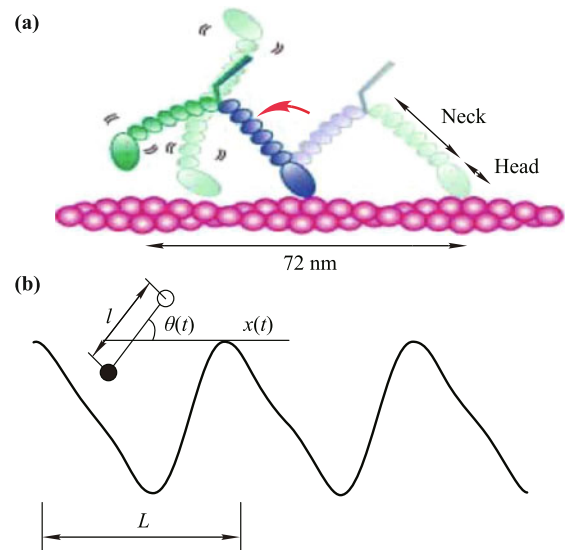


Fig. 1 (a) Postulated walking scheme for myosin V from Ref. [6]. (b) Sketch of the dimer with translational and rotational degrees of freedom. It is depicted as particle 1 (the black one) and particle 2 (the white one) connected by a rod of length l . The potential contours of the dimensionless double-sine potential in Eq. (1) shown in the lower graph is periodic in the spatial coordinate with period L and exhibits a broken spatial symmetry. Parameters used were $L = 1$, $U_0 = 1$.

The potential energy of the motor is determined by the locations of those two heads and the orientation of the motor. Since the filament is periodic, the potential along the translational direction is a periodic asymmetric ratchet potential as

$$U_x(x) = U_0 \left[\frac{1}{2} \sin\left(\frac{2\pi x}{L}\right) + \frac{1}{8} \sin\left(\frac{4\pi x}{L}\right) \right] \quad (1)$$

where U_0 is the dimensionless amplitude of the ratchet potential and L is the distance between the two minima, $U_x(x) = U_x(x + L)$.

In general, it is simple enough to limit the motor in a channel though setting y direction in a parabolic potential, like $U_y(y) = \omega_y y^2/2$. The motors hydrolyze ATP and release the energy during a biochemical cycle, the rotational angle would be changed continuously depending on time. Smaller motions and rotations of the lever arm have been associated with ADP release from the trailing head [20]. Additional small steps and lever arm rotations were detected when the leading-head lever arm stroked before [21] or after [22] the trailing head detached. Therefore, the rotation angle could be locally oscillating or continuously rotating. We assume a cosine potential in θ -direction for simplicity,

$$U_\theta(\theta) = U_{rot} \cos(\theta + \varphi) \tag{2}$$

U_{rot} is the dimensionless amplitude of the cosine potential and φ is the initial phase which is usually defined as zero.

The total potential energy of the motor from the filament as a function of x and θ is given by

$$V(x, \theta) = U_x(x) + U_\theta(\theta) \tag{3}$$

Since most of the molecular motor transport occurs in the overdamped regime, we can safely neglect inertial effects [23–26]. Thus, the motion of the dimer is described as a whole with the following equations:

$$\gamma_x \frac{dx}{dt} = -\frac{\partial V(x, \theta)}{\partial x} \tag{4}$$

$$\gamma_\theta \frac{d\theta}{dt} = F - \frac{\partial V(x, \theta)}{\partial \theta} + \xi(t) \tag{5}$$

where x is the position for the center of mass, θ is the rotation angle (see Fig. 1), γ_x and γ_θ are the friction constants in translational and rotational directions, respectively. F is an external driving force which could induce the continuous rotation of the dimer and the auxiliary variable $\xi(t)$ represents the coupling of the dimer to the environment and the environmental fluctuations. It is modeled by a Gaussian white noise define with $\langle \xi(t) \rangle = 0$ and autocorrelation function

$$\langle \xi(t)\xi(s) \rangle = 2D_\theta \delta(t - s) \tag{6}$$

with D_θ is the noise intensity of the statistically independent noises in rotation direction. To reduce the number of parameters, we use dimensionless units only. Accordingly, after simple algebra (the friction coefficient is absorbed into the time unit), Eqs. (4) and (5) become

$$\dot{x} = -\frac{\pi U_0}{2L} \left(2 \cos \frac{2\pi x}{L} \cos \frac{\pi l \cos \theta}{L} + \cos \frac{4\pi x}{L} \cos \frac{2\pi l \cos \theta}{L} \right) \tag{7}$$

$$\dot{\theta} = F - \sin \theta + \xi(t) \tag{8}$$

For zero thermal noise, Eq. (8) has the same form as the Adler equation [27].

The main interest in this article will be the mean current of the center of mass in x -direction, which is the time average of the average velocity over an ensemble of initial conditions,

$$J_x = \lim_{t \rightarrow \infty} \left\langle \frac{x(t) - x(0)}{t} \right\rangle \tag{9}$$

where the brackets denote averaging over different realizations of the noise. As there is no analytical method to handle these situations effectively, we carried out extensive numerical simulations. We have numerically integrated Eqs. (7) and (8) by the fourth-order Runge–Kutta algorithm. Examining the trajectories of numerous motors allows us to determine the average behavior of the system. We have chosen the following constant parameter values which will be used throughout the current study: $U_0 = 1$, $U_{rot} = 1$ and $L = 1$. For our purposes, the simulations are performed an average over 100 trajectories for velocities, the time step $\Delta t = 0.001$ and each single trajectory covers a time span of 10^4 dimensionless time units.

3 Deterministic current behavior

A dimer such as the one described above moving in a periodic asymmetric ratchet potential like Eq. (1) in the absence of thermal fluctuations, exhibits no directional motion. However, such motion can be induced by the external force in the rotational direction. The numerical results show that only appropriate driving force could produce nonzero current and there exists an optimal driving value to determine the maximum current. In Fig. 2 we plot the current J_x as function of F for $D_\theta = 0$. According to the analysis of dynamic, directional motion exists only if $|F| > 1$ in the absence of thermal fluctuations, or else the system will stay in a fixed point.

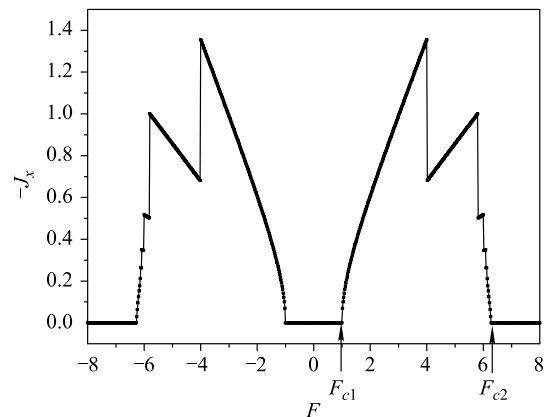


Fig. 2 Current J_x vs. external force F . Parameter values: $l = 1.0$, $D_\theta = 0$.

Note that there is net directional flux in negative direction when $F_{c1} < F < F_{c2}$, as can be seen from Fig. 2. The lower threshold F_{c1} corresponds to the force that is needed to overcome the barrier of the cosine potential in the rotational direction. Except for the case of $|F| < |F_{c1}|$, the net flux also locks into zero for large driving force ($|F| > |F_{c2}|$). Obviously, the results of positive F are symmetrical with the case of negative F as $\cos \pi l \cos \theta / L$ is an even function in Eq. (7). For this reason, we only need to discuss the positive F case in the following part.

In addition, the behavior of the current in Fig. 2 also indicates some transitions as the force is increasing to a large value. For a detailed analysis we need to investigate the walking patterns of the dimer. Figure 3 shows the positions of the two particles as a function of time which are computed for different values of load force in the same time interval. During one step the two heads approach each other in translational direction and then separate again, while their order can change alternately. A change in the rotation velocity $\dot{\theta}$ enables the motor to

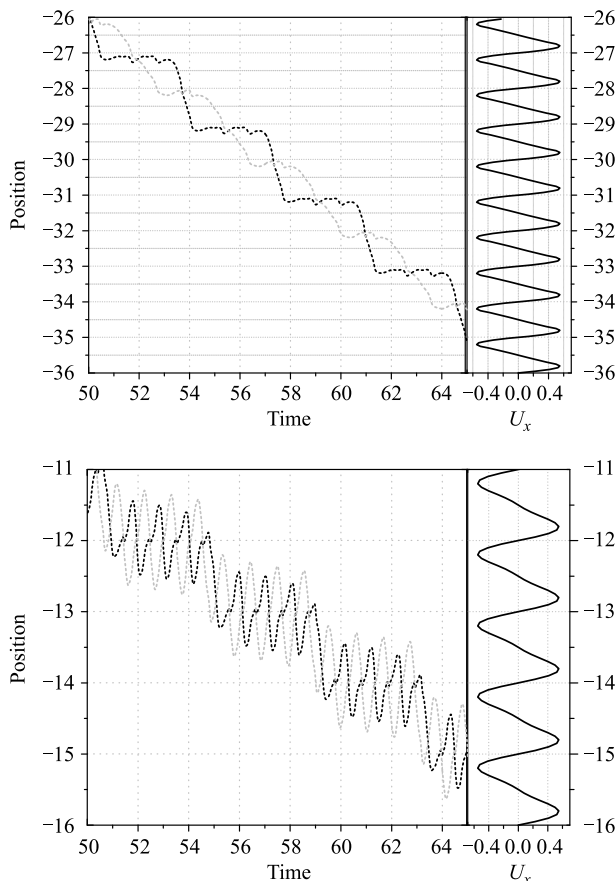


Fig. 3 Example trajectories for two different force. we identify the position of particle 1 and the position of particle 2 with gray dot line and black dot line. $F = 2.0$ in the upper part and $F = 6.0$ in the lower part. The right curve in each part is the corresponding potential in x -direction. Parameter values: $l = 1.0$, $D_\theta = 0$.

rotate several cycles in a potential periods until it is large enough to traverse to the basin of attraction of the next well. These numerical simulations actually reproduce the expected mechanism, a “hand-over-hand” net advance of the molecule which is also proved in other models [28, 29] and there is strong evidence that kinesin also moves in such manner [3, 30]. We notice that there is qualitative difference between the trajectory for the case of small force $F = 2.0$ and large one $F = 6.0$. Larger force makes the dimer could rotate more times in a potential barrier, see the lower part of Fig. 3. Also, in the latter case, the particles requires much more time to traverse one well in the ratchet potential.

In order to explain the transitions theoretically, we calculate the characteristic exponents (or Floquet exponents) of the limit cycle γ_0

$$\gamma_0 = \frac{1}{T} \int_0^T \{2\pi^2 [\sin(2\pi x) \cos(\pi l \cos \theta) + \sin(4\pi x) \cos(2\pi l \cos \theta)] + \cos \theta\} dt \quad (10)$$

and the transition happens only if when $\gamma_0 = 0$. To show the occurrence of the transition, we plot the current J_x vs F curve and the relationship between γ_0 and F in Fig. 4. We see the transition happens when the characteristic exponents γ_0 approaches to zero.

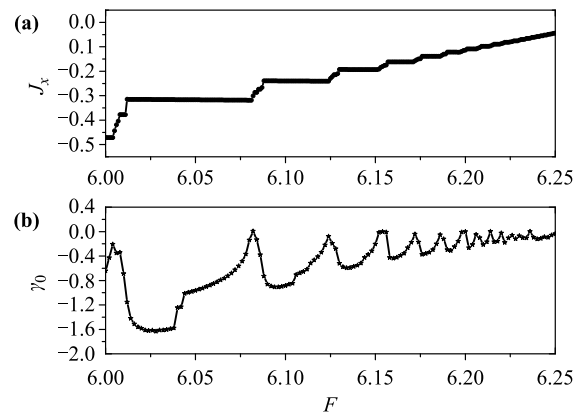


Fig. 4 (a) Current J_x - F curve which use the same parameter values as in Fig. 2. (b) The characteristic exponents of the numerical simulations as a function of F in Eq. (10).

The agreement between the force value for the current transition determined by Eq. (9) and the theoretical calculating value γ_0 proves that the limit cycle collapse causes the dimer traverse to the basin of attraction of the next well. Therefore, we could get the conclusion that the collapse of the limit cycle stability leads to the transition.

4 Stochastic dynamic behavior

The deterministic ratchet problem is a good starting

point for analyzing the system in the presence of thermal noise. We now investigate the effect of noise. In general the translational diffusion alone is too small to generate directed motion. The current here arises as a consequence of both the external force and noise in the rotational direction.

Numerical simulations of the current depending on the external force obtained with different values of the noise intensity parameter D_θ are shown in Fig. 5. Observe that the behavior of the current when $D_\theta = 0$ and $D_\theta \sim 0$ display similar features, the noise is smoothing the transitions. In the presence of thermal fluctuations the noise-induced current exhibits many interesting features. There are two distinct regimes which will be discussed in the following section: (i) small D_θ and small external force F , there exists resonance district; (ii) large D_θ and no external force $F = 0$, there is directional current and even current reversal when the noise strength is getting larger.

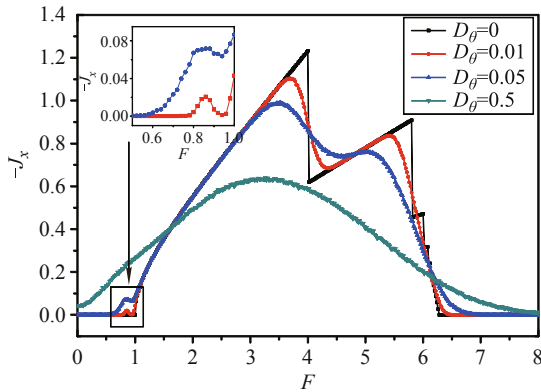


Fig. 5 Current J_x vs. F for $D_\theta = 0$, $D_\theta = 0.01$, $D_\theta = 0.05$, and $D_\theta = 0.5$ (From top to bottom). Parameter values, $l = 1.0$. Inset: Enlargement of the small-force regime for $D_\theta = 0.01$ and $D_\theta = 0.05$.

We first study case (i), examining the effect of noise in the interplay of small noise and external force. From the inner figure of Fig. 5 we can observe a resonance-like peak in the regime $F < 1$, which is denoted as F_0 . The value of F_0 does not change even with different small D_θ . It is worth emphasizing that the role of external force is more important in the presence of small noise, and the corresponding relatively regular injection of energy “quanta” also defines an approximate time scale that gives rise to resonance-like phenomena. We change the length of the rod l and the results exhibit several resonance-like peaks when $l > 1$, see the lower graph of Fig. 6.

To study these effects theoretically, we now turn to the stochastic process described by the Langevin equation (8) which could be alternatively written in term of

the probability density $P(\theta, t)$ that satisfies the following Fokker–Plank equation [31]:

$$\frac{\partial P(\theta, t)}{\partial t} = -\frac{\partial}{\partial \theta}(F - \sin \theta)P(\theta, t) + D_\theta \frac{\partial^2}{\partial \theta^2}P(\theta, t) \quad (11)$$

This equation is complemented by natural boundary conditions $P(x, t) \rightarrow 0$. An exact analytic solution of Eq. (11) seems impossible. After initial transients have died out, we get the stationary solution as $t \rightarrow \infty$ in the condition that $|F| \leq 1$ and $D_\theta \rightarrow 0$,

$$P_{st}(\theta) = \delta(\theta - \arcsin F) \quad (12)$$

with

$$\frac{\partial P_{st}}{\partial t} = 0 \quad (13)$$

then

$$\langle \cos \theta \rangle_{D_\theta \rightarrow 0} = \sqrt{1 - F^2}, \quad |F| \leq 1 \quad (14)$$

Considering the dimer dwells in the potential wells in most time in the presence of small noise, the velocity near the potential well is exactly crucial to the average current. We get the velocity of the particle in the potential well from Eq. (7) which would have the form of the parabola equation. Because of $\cos(\pi l \cos \theta) \in [-1, 1]$, it is easy to get the maximum velocity of the center of mass when we take some value a_0 for $\cos(\pi l \cos \theta)$. Here, the potential U_x is spatially periodic, so

$$l \cos \theta = \arccos(a_0)/\pi + 2k \simeq 0.42 + K, \quad K = 0, 1, \dots, N \quad (15)$$

Then we could estimate the resonance peak F_0 from Eq. (14) and Eq. (15),

$$F_0 = \sqrt{1 - \left(\frac{0.42 + K}{l}\right)^2} \quad (16)$$

For different values of the rod length l , the resonance peaks of the current in the case of small force and weak noise occur more than once. The estimation values of Eq. (16) in the upper part of Fig. 6 coincide precisely with the numerical results of Eq. (9) in the lower part for the parameter $l = 5.5$.

Without the external force the numerical evaluation of the current as a function of the noise intensity D_θ yields a rich behavior, featuring an amazingly steep current reversal, see Fig. 7. Note that the direction of the net current shows highly nonintuitive behavior. The directed current first increases with increasing D_θ , reaches a maximum and then decreasing with D_θ . On further increasing D_θ after $D_{\theta 0}$ the current reverses to the other direction.

There are two main physical mechanisms who govern

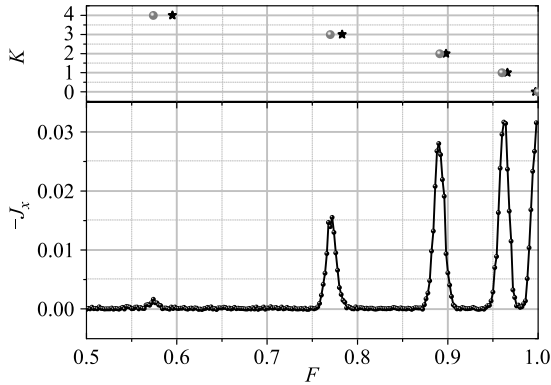


Fig. 6 The lower part is the current J_x -force F relation for $l = 5.5$, while the upper part is the corresponding estimation value of F from Eq. (16) under the condition of take K from 1 to 5.

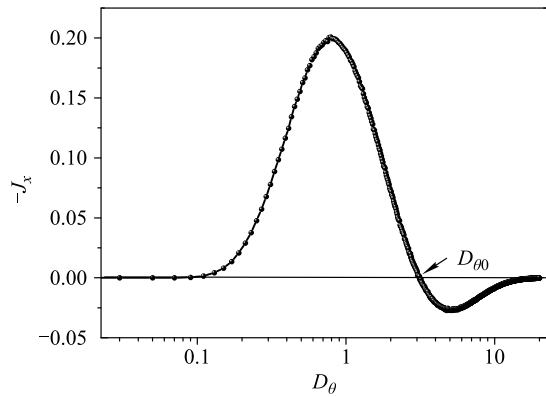


Fig. 7 Current J_x vs. thermal noise strength D_θ for the following parameter values in Eqs. (7) and (8): $U_0 = 1$, $U_r = 0$, $L = 1$, $F = 0$. The current in this case becomes positive for sufficiently large noise strength.

the occurrence of current reversal: the noise-induced positive motion and the ratchet effect. The direction of the directed transport is determined by the interplay of the potential geometry and thermal fluctuations. Observe that the system shows a current reversal for large noise and the current vanishes at very high noise strength, the effect of the potential is drowned out by the noise in this case. The mechanism of the current reversal differs distinctly from the case in Ref. [32]. A satisfying (analytical) explanation has not been found.

In the preceding section presented we have proposed that there is only thermal noise in rotation direction and no thermal noise in translational direction. Here, we will explain why we have to give this assumption. We shall first try to add thermal noise in both degrees of freedom. It is further assumed that these noises are independent random variables. Rewrite Eqs. (7) and (8) as

$$\dot{x} = -\frac{\pi U_0}{2L} \left(2 \cos \frac{2\pi x}{L} \cos \frac{\pi l \cos \theta}{L} \right. + \cos \frac{4\pi x}{L} \cos \frac{2\pi l \cos \theta}{L} \left. \right) + \xi_1(t)$$

$$+ \cos \frac{4\pi x}{L} \cos \frac{2\pi l \cos \theta}{L} + \xi_1(t) \tag{17}$$

$$\dot{\theta} = F - \sin \theta + \xi_2(t) \tag{18}$$

where $\xi_1(t)$ and $\xi_2(t)$ are independent δ -correlated Gaussian white noises with zero average and the correlation function

$$\langle \xi_i(t) \rangle = 0 \tag{19}$$

$$\langle \xi_i(t) \xi_j(s) \rangle = 2D_i \delta(t-s) \delta_{ij}, \quad i = 1, 2 \tag{20}$$

As indicated in Eqs. (19) and (20), we distinguish between D_1 and D_2 being the intensities of the noise sources in the dynamics for \dot{x} and $\dot{\theta}$. The ratio of D_1 and D_2 can be merged into a dimensionless parameter α , allowing us to define $D_\theta = D_2$ and $\alpha := D_1/D_2$.

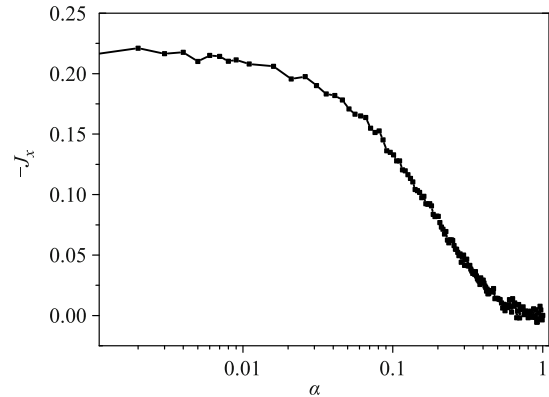


Fig. 8 Current J_x as a function of the dimensionless parameter α . Parameter values: $l = 0$, $D_2 = 0.8$, and $F = 0$.

Since the current has the optimal value in $D_2 = 0.8$ to get the maximum current when $D_1 = 0$ (see Fig. 7), we set D_2 as a constant parameter to obtain Fig. 8. In the case of $D_1 \neq D_2$, Fig. 8 shows that the smaller the α the stronger the directed current is. One observes a obvious negative current when the ratio is extremely small, while a further increase of noise density D_1 suppress the influence of the noise effect and the asymmetric ratchet potential. The current decreases to zero when D_1 could be compared with D_2 . It proved that the mainly effective noise to induce the resulting directed transport is ξ_2 in the rotational direction. The rotational diffusion plays a more significant role than the translational diffusion.

5 Conclusions

In our work, a model that describes the motion of a two-head dimer in a ratchet potential is proposed. Through cooperation particles could transfer energies from rotational direction to the transport in the translational direction. Without any directed force and additional ther-

mal noise in the translational direction, these models perform directional transport. The rotation of a dimer and a proper asymmetric potential are enough to produce the macroscopic motion of the particles toward particular direction.

The behavior of the current depends sensitively on system parameters such as external force F and noise strength D_θ which exhibit several novel features. There exists an optimal value of driving force and there are several transitions with increasing external force. An analysis of stability analysis of limit cycles is applied to explain the occurrence of these transitions.

In the presence of thermal fluctuations the noise could smooth those transition peaks in the J_x-F curve. In the case of small force we found resonance-like peak which depends sensitively on the length of the rod. Without the external force the thermal noise in the rotational direction could also induce directed current and we have also observed current reversals as noise strength is getting larger. Besides, we also explained why we have to add noise in the rotational direction rather than the translational direction.

In conclusion, we have developed a realistic model of motor proteins which could simulate physically their cooperative directed transport in a “hand-over-hand” fashion. The properties of this model are qualitatively consistent with recent experimental results. This rotation-translation coupling model give us a simpler and feasible perspective to understand the motion mechanism of the motor proteins, no matter the myosin superfamily or other molecular motors such as kinesin.

Acknowledgements We thank Peter Hänggi for valuable discussions. This work has been financially supported by grants from the National Natural Science Foundation of China (Grant No. 11075016) and the Foundation for Doctoral Training from Ministry of Education (Grant No. 20100003110007).

References

1. A. Yildiz, J. N. Forkey, S. A. McKinney, T. Ha, Y. E. Goldman, and P. R. Selvin, Myosin V walks hand-over-hand: Single fluorophore imaging with 1.5-nm localization, *Science*, 2003, 300(5628): 2061
2. A. Yildiz, H. Park, D. Safer, Z. Yang, L. Q. Chen, P. R. Selvin, and H. L. Sweeney, Myosin VI steps via a hand-over-hand mechanism with its lever arm undergoing fluctuations when attached to actin, *J. Biol. Chem.*, 2004, 279(36): 37223
3. A. Yildiz, M. Tomishige, R. D. Vale, and P. R. Selvin, Kinesin walks hand-over-hand, *Science*, 2004, 303(5658): 676
4. S. L. Reck-Peterson, A. Yildiz, A. P. Carter, A. Gennerich, N. Zhang, and R. D. Vale, Single-molecule analysis of Dynein processivity and stepping behavior, *Cell*, 2006, 126(2): 335
5. M. von Delius and D. A. Leigh, Walking molecules, *Chem. Soc. Rev.*, 2011, 40(7): 3656
6. K. Shiroguchi and K. Kinoshita, Myosin V walks by lever action and brownian motion, *Science*, 2007, 316(5828): 1208
7. A. R. Dunn and J. A. Spudich, Dynamics of the unbound head during myosin V processive translocation, *Nat. Struct. Mol. Biol.*, 2007, 14(3): 246
8. F. Jülicher, A. Ajdari, and J. Prost, Modeling molecular motors, *Rev. Mod. Phys.*, 1997, 69(4): 1269
9. R. D. Astumian, Thermodynamics and kinetics of a Brownian motor, *Science*, 1997, 276(5314): 917
10. M. Dittrich, J. Yu, and K. Schulten, PcrA Helicase, a molecular motor studied from the electronic to the functional level, in: *Atomistic Approaches in Modern Biology*, edited by M. Reiher, Springer, 2007, pp. 319–347
11. Z. G. Zheng, G. Hu, and B. Hu, Collective directional transport in coupled nonlinear oscillators without external bias, *Phys. Rev. Lett.*, 2001, 86(11): 2273
12. Z. G. Zheng, M. C. Cross, and G. Hu, Collective directed transport of symmetrically coupled lattices in symmetric periodic potentials, *Phys. Rev. Lett.*, 2002, 89(15): 154102
13. H. B. Chen, Q. W. Wang, and Z. G. Zheng, Deterministic directed transport of inertial particles in a flashing ratchet potential, *Phys. Rev. E*, 2005, 71(3 Pt 1): 031102
14. Z. G. Zheng and H. B. Chen, Cooperative two-dimensional directed transport, *Europhys. Lett.*, 2010, 92(3): 30004
15. H. B. Chen and Z. G. Zheng, Deterministic collective directional transport in one-dimensional flashing ratchet potentials, *Mod. Phys. Lett. B*, 2011, 25(14):1179
16. B. Alberts, D. Bray, J. Lewis, M. Raff, K. Roberts, and J. D. Watson, *Molecular Biology of the Cell*, New York: Garland Publishing Comp., 1983
17. S. von Gehlen, M. Evstigneev, and P. Reimann, Dynamics of a dimer in a symmetric potential: Ratchet effect generated by an internal degree of freedom, *Phys. Rev. E*, 2008, 77(3): 031136
18. D. Dan, A. Jayannavar, and G. I. Menon, A biologically inspired model for two-headed Brownian motors, *Physica A*, 2003, 318: 40
19. B. Geislinger and R. Kawai, Brownian molecular motors driven by rotation-translation coupling, *Phys. Rev. E*, 2006, 74(1): 011912
20. C. Veigel, F. Wang, M. L. Bartoo, J. R. Sellers, and J. E. Molloy, The gated gait of the processive molecular motor, myosin V, *Nat. Cell Biol.*, 2001, 4(1): 59
21. G. Cappello, P. Pierobon, C. Symonds, L. Busoni, J. Christof, M. Gebhardt, M. Rief, and J. Prost, Myosin V stepping mechanism, *Proc. Natl. Acad. Sci. USA*, 2007, 104(39): 15328
22. S. Uemura, H. Higuchi, A. O. Olivares, E. M. De La Cruz, and S. Ishiwata, Mechanochemical coupling of two substeps in a single myosin V motor, *Nat. Struct. Mol. Biol.*, 2004, 11(9): 877

23. J. Prost, J. F. Chauwin, L. Peliti, and A. Ajdari, Asymmetric pumping of particles, *Phys. Rev. Lett.*, 1994, 72(16): 2652
24. J. Rousselet, L. Salome, A. Ajdari, and J. Prost, Directional motion of brownian particles induced by a periodic asymmetric potential, *Nature*, 1994, 370(6489): 446
25. M. O. Magnasco, Forced thermal ratchets, *Phys. Rev. Lett.*, 1993, 71(10): 1477
26. R. D. Astumian and M. Bier, Fluctuation driven ratchets: Molecular motors, *Phys. Rev. Lett.*, 1994, 72(11): 1766
27. R. Adler, A study of locking phenomena in oscillators, *Proceedings of the IRE*, 1946, 34(6): 351
28. F. Falo, J. Munárriz, and J. Mazo, Model for hand-over-hand motion in molecular motors, *Statistical Mechanics of Molecular Biophysics*, 63(2008)
29. A. G. Hendricks, B. I. Epureanu, and E. Meyhöfer, Collective dynamics of kinesin, *Phys. Rev. E*, 2009, 79(3): 031929
30. C. L. Asbury, A. N. Fehr, and S. M. Block, Kinesin moves by an asymmetric hand-over-hand mechanism, *Science*, 2003, 302(5653): 2130
31. H. Risken, *Fokker–Planck Equation*, Springer, 1984
32. P. Reimann, R. Bartussek, R. Häußler, and P. Hänggi, Brownian motors driven by temperature oscillations, *Phys. Lett. A*, 1996, 215(1–2): 26